https://doi.org/10.1016/j.conbuildmat.2021.125063

Concrete reinforced with macro fibres recycled from waste GFRP

Bing FU[1,2,3], K.C. LIU[3], J.F. CHEN[4,5] and J.G. TENG[3,*]

[1] School of Mechanics and Construction Engineering, Jinan University, Guangzhou 510632, China
[2] MOE Key Lab of Disaster Forecast and Control in Engineering, Jinan University, Guangzhou 510632, China
[3] Department of Civil and Environmental Engineering, The Hong Kong Polytechnic University, Hong Kong, China
[4] Department of Ocean Science and Engineering, Southern University of Science and Technology, Shenzhen 518000, China
[5] Southern Marine Science and Engineering Guangdong Laboratory (Guangzhou), Guangzhou 511458, China

Abstract: Fibre reinforced polymer (FRP) composites are widely used in many industries due to their excellent mechanical and durability properties. This means that an increasing amount of FRP waste, arising from production, processing and decommissioning, needs to be processed. Common FRP composites are normally thermoset and non-biodegradable, posing a significant environmental threat if they are not disposed of properly at their end of life. While recycling of FRP is environmentally desirable, almost all existing recycling methods, which are based on either thermal, chemical or mechanical processes, are economically unviable if governmental subsides are not available. The recycling of glass FRP (GFRP) waste, which accounts for over 95% of all types of FRP waste by weight, is even more economically challenging than the recycling of carbon FRP (CFRP) waste due to the lesser economic value of the former. This paper explores a novel mechanical method for recycling GFRP waste by processing it into macro fibres for reinforcing concrete, with the resulting material referred to as macro fibre reinforced concrete (MFRC). The mechanical properties of MFRC were investigated. The test results showed that the addition of macro fibres had two major effects on the concrete: (1) the workability of concrete depends strongly on the macro fibre volume ratio, with the slump value reducing from 176 mm to 83 mm as the macro fibre volume ratio increased from 0% to 1.5%; (2) the flexural strength and toughness of the concrete be greatly enhanced by the addition of macro fibres, e.g., by 1.3 and 230 times when the macro fire value ratio was 1.5%. The proposed recycling method for waste GFRP is therefore believed to be both technically feasible and economically attractive.

Keywords: GFRP; waste; mechanical recycling; macro fibre; concrete.

* Corresponding author. Email: cejgteng@polyu.edu.hk

Introduction

Fibre reinforced polymer (FRP) composites are widely used in industries such as aerospace, automotive, marine and construction due to their highly favourable properties, including their high strength-to-weight ratio and excellent corrosion and fatigue resistance [1]. The global FRP composite production, of which 95%-98% in weight is glass FRP (GFRP) composites, and 75% in weight is thermosets, is expected to increase from 10.4 million tonnes in 2015 to 12.9 million tonnes in 2021, at an average annual growth rate of about 4%[2]. Inevitably, an increasing amount of FRP composite waste arises from the manufacturing (e.g., leftover bits and pieces of fibres during the pultrusion process), processing (e.g., cut-off pieces of FRP bars to fit desired lengths), or decommissioning at the end of service life. As almost all types of thermoset FRP waste are non-biodegradable, they pose an important environmental challenge that has attracted increasing attention but the development of practical recycling methods is still in its infancy[3-6].

A variety of approaches have been explored to deal with FRP waste, mainly including landfilling, incineration and recycling. Landfilling currently remains the simplest and most economically viable method to deal with FRP waste, especially for GFRP waste. The cost of landfilling each tonne of solid waste was estimated to range from US$45 to $200 in 2014 in the US [6] and from £120 to £130 in 2017 in the UK[5]. Landfilling as a waste processing method faces increasing difficulties: a higher tax rate is likely to be levied and relevant legislations are becoming more stringent. For example, the European Commission revised its Landfill Directive in 2018, aiming at reducing the amount of municipal waste sent to landfill sites to 10% or less by 2035[7]. In a congested place like Hong Kong, landfill sites are particularly difficult to secure, and the current sites are expected to be exhausted soon [8]. Incineration is even less popular owing to toxic emissions during the combustion process, although some energy in the FRP matrix is recovered. Moreover, after the incineration of the FRP waste, approximately 50-70% in weight is left as ash, which still needs to be landfilled [3,4].

Recycling, which typically involves a thermal, chemical or mechanical process, is a more environment-friendly method for managing various FRP wastes. The economic feasibility of different recycling routes depends on not only the recycling method itself but also the components of the FRP waste. It is more challenging to recycle GFRP waste economically than carbon FRP (CFRP) waste because of the lower value of recycled glass fibres, whose properties also degrade at high temperatures [4,5]. Therefore, both thermal and chemical-based methods have been considered to be economically unviable for recycling GFRP[5,6].

Co-processing of GFRP waste in cement kilns has been widely investigated and has been recommended by the European Composites Industry Association[9]. In such a process, the GFRP waste is fed into the kiln in which the resin is burnt to provide heat

energy, and the glass fibres are reduced to cement clinkers. This route is relatively simple, and is therefore commercially active in some countries (e.g., Japan, Germany, Denmark and U.K.) [3,10]. However, the cost of transporting and processing GFRP waste is usually significant, which means that this option is often less economically attractive than landfilling at a local site if it is permitted.

In addition to co-processing in cement kilns, another potentially economically viable route is a mechanical process, through which the GFRP waste is processed by shredding, crushing or milling into powder or fibrous products or both, which can be used as fillers or reinforcements in construction materials and other products (e.g.,[6,11-15]). A number of studies have been conducted to explore the feasibility of using such products from GFRP waste to replace fine or coarse aggregate in cementitious materials (e.g.,[11,12,16-18]). However, the studies have shown that the addition of powders from GFRP waste into concrete as partial replacement of fine aggregate resulted in significant reductions in the mechanical properties of the hardened concrete. For instance, Asokan et al. [11]found that the compressive strength of concrete was reduced by as much as 60%, when 50% of the fine aggregate in weight was replaced by a GFRP waste powder. Correia et al. [12] conducted a similar study and found that a 5-20% replacement of the fine aggregate in volume resulted in reductions of up to 47% in the cylinder compressive strength. Yazdanbahksh et al. [17] cut GFRP reinforcing bars into short cylinders (with a length-to-diameter ratio of around 1), which were then used to partially or fully replace coarse aggregate in concrete. Compared with the grinding of FRP waste into powder, cutting scrap FRP bars into such short cylinders requires much less energy. They observed that the compressive and tensile strengths were respectively reduced by up to 21% and 35% when the natural coarse aggregate was fully replaced by the GFRP short cylinders. Alam et al. [19] used small prisms (i.e., referred to as FRP scraps herein) cut from long strips of waste FRP to replace coarse aggregate at different ratios (25% and 50% in volume). These FRP scraps had similar gradations to those of the natural coarse aggregate to be replaced. Their test results showed that replacing the natural coarse aggregate with the FRP scrap aggregate reduced the compressive and the flexural strengths by up to about 40% and 38% respectively. It should be noted that the FRP scraps in their study were coated with a thin layer of gel. This coating is expected to have made the FRP scraps smooth and amplified their detrimental effect on the mechanical properties of concrete.

In contrast to reductions in mechanical properties as a result of the addition of processed GFRP waste powder and short scraps into concrete, incorporating fibres or slender forms of reinforcement recycled from GFRP waste has been found to enhance the mechanical properties, especially the tensile and flexural strengths, of concrete. Asokan et al. [11] found that incorporation of waste fibres of 5% in volume into cladding panels increased their flexural strengths by up to 46%. García et al. [14] exploited various mechanical processes which combine shredding, milling and sieving in different

manners to produce short fibres from GFRP waste. They reported that with the simple addition of short fibres of 1% in weight, the greatest enhancements in the compressive and flexural strengths of the concrete were respectively 26% and 16%. Yazdanbakhsh et al. [18,20,21] incorporated slender reinforcing elements, which were cut from GFRP bars or wind turbine blades, and referred to as "FRP needles" (with a length-to-diameter ratio of about 17), to replace 5% and 10% of coarse aggregate in concrete. Their test results showed that incorporation of FRP needles significantly increased the energy absorption capacity under both compression and tension, but slightly reduced the compressive strength of concrete. Similar conclusions have recently been reached by Dong et al. [22], who added BFRP needles to sea-sand concrete. Their results showed that both the splitting tensile strength and the flexural strength were increased by up to 32% and 14% when 5-20% of coarse aggregate was replaced by BFRP needles. Nie et al. [23] conducted a series of tests on full-scale RC beams to investigate the effect of GFRP needles as partial replacement of coarse aggregate in concrete on the shear behaviour of RC beams. Their results showed that the partial replacement of 5% or 10% led to an enhancement of 30-40% in the total energy absorbed by the RC beams during the failure process but had a very limited effect on the shear capacity.

From the above review, it may be concluded that the addition of either powder or fibres mechanically processed from GFRP waste into concrete leads to a reduction or a small increase in the mechanical properties. As a result, the existing mechanical recycling processes are not very attractive as the GFRP waste products included in concrete function mainly as a filler material that is more likely to have a detrimental rather than beneficial effect on the properties of concrete.

This paper presents a new method of mechanical recycling of FRP wastes into small reinforcing elements called "macro fibres" for concrete, and the effects of including such macro fibres into concrete on its mechanical properties. A decommissioned GFRP wind turbine blade was used to produce macro fibres in the present study. Nonetheless, the method is readily applicable to many other types of FRP wastes. These macro fibres are defined, for the purpose of the present study, to have a typical thickness similar to that of a lamina (e.g., 0.4-1.0 mm), a width of several millimetres, and a length of 30-100 mm, leading to an aspect ratio (i.e., the length-to-thickness ratio) of 30-120, which is close to that of common steel fibres used in concrete [24].

Production of Macro Fibres from a Decommissioned GFRP Wind Blade

The macro fibres used in the present study were mechanically recycled from a decommissioned wind blade using a process as illustrated in Figure 1. The wind blade,

which was approximate 30 m long, was first cut into several large segments in the wind power plant and then transported to a local factory. These large segments were further cut in the local factory into smaller segments of 1 to 2 m long. These smaller segments were next saw-cut into strips (referred to as macro fibres) with the following intended dimensions: a length of about 90 mm, a width of about 3 mm, and a thickness similar to that of the lamina of the wind turbine (the thinnest value that could be practically achieved using the available machine). The width of macro fibres has effect on two aspects: (1) the aspect ratio of macro fibre cross-sections, but the effect of aspect ratio would be negligible if the width of macro fibres is much greater than their thickness; (2) the number of macro fibres from the same amount of FRP waste, which has a negligible effect on the mechanical performance of an MFRC specimen that contains a sufficient number of macro fibres. As a result, the width of the macro fibres used in the present study was chosen to be 3 mm to facilitate the cutting process of the macro fibres and ensure that a sufficient number of macro fibres was present in each specimen. Note that the macro fibre production procedure as executed in the present study was time-consuming and labour-intensive, but the purpose of this study was to investigate the feasibility and attractiveness of the recycling method. For industrial-scale applications, this process can be improved and automated using a properly designed machine.

The actual dimensions of the manufactured macro fibres were measured and analysed for 300 samples randomly chosen from a pile of macro fibres. Their mean values of length, width and thickness were 89.7 mm, 3.04 mm and 0.79 mm with corresponding standard deviations of 3.67, 0.74 and 0.20 respectively, giving an aspect ratio of about 114, which is close to the upper limit of 120 defined above for macro fibres. The frequency distributions of the length, width and thickness of the macro fibres are presented in Figure 2, where normal distributions with the same mean values and standard deviations are shown for reference.

Mechanical recycling requires much less energy than chemical recycling or thermal recycling [5,6]. The proposed recycling method generates a much smaller total surface area than grinding into power or shredding into smaller reinforcing elements, thus leading to the consumption of less energy than recycling methods based on gridding and shredding. Not much powder waste (less than 10% of the total waste volume according to the present study) is produced by the macro fibre production procedure, mainly because the macro fibres contain both fibres and resin. Such a small amount of powder waste can be easily handled using different methods (e.g., as filler of a small volume fraction in concrete, asphalt-concrete and other products) without causing a significant detrimental effect. As a result, the processing method itself is attractive in terms of processing cost and the small amount of “un-useable” powder waste resulting from it.

Experimental Program on MFRC

Concrete mix proportions

Four concrete mixes as listed in Table 1 were adopted. The only variable among them was the amount of macro fibres as the main aim of this study was to investigate the effect of macro fibres on the properties of the concrete. The volume fractions of macro fibres in these mixes were 0, 0.5%, 1.0%, and 1.5%. The amount of macro fibres in weight for each batch of concrete was calculated based on the design volume fraction and the measured density of 1970 kg/m^3 for the macro fibres. The different batches of concrete produced from these mixes are designated CC, MFRC0.5, MFRC1.0 and MFRC1.5 respectively. River sand and crushed granite of 20 mm in maximum particle size was used as the fine and the coarse aggregates respectively, and Type I Portland cement was used in all the concrete mixtures. Both the aggregates and the macro fibres were left to dry under direct sunshine before they were used in casting the concrete, and therefore the moisture in these materials was neglected. The fact that the water absorption capacities of the aggregates and the macro fibres were not measured does not have significant implications for the purpose of the present study as exactly the same constituent materials and proportions (except the amount of macro fibres) were used in preparing the concrete, and therefore the effect of the volume fraction of macro fibres could still be properly examined. It should however be noted that if a concrete mix needs to be designed to closely achieve a target strength, the water absorption capacities of the constituent materials need to be precisely known. In the present study, the control group (mix CC), without macro fibres, was designed to have a target cylinder compressive strength of 40 MPa and a slump of 180 mm; the actual average cylinder compressive strength achieved was 45.7 MPa while the actual slump value was 176 mm.

Specimen Preparation and Test Methods

For each type of concrete, eight cylinders with a diameter of 150 mm and a height of 300 mm, and four prismatic beams of 150 mm x 150 mm x 550 mm were prepared. All these specimens were cast from a single batch of concrete to ensure consistency. The size of beam specimens used in this study was the larger of the two preferred sizes given in ASTM C1609 [25]. The size of test specimens affects the orientation and distribution of macro fibres near the internal surfaces of the mould; therefore, it is common for standards for testing fibre reinforced concrete (FRC) beams (e.g., [25,26]) to specify that the beam width and depth should be larger than three times the maximum fibre length. However, this requirement can be waived for beam moulds with the larger of the two preferred sizes when long fibres are used according to ASTM C1609 [25].

The concrete was mixed following the Hong Kong design code for concrete structures [27]. The macro fibres were gradually added during the mixing process to ensure that they would be evenly distributed. Before casting the specimens, a slump test in accordance with ASTM C143 [28] was conducted to investigate the effect of macro fibres on concrete workability. All specimens were demoulded 24 hours after casting and then cured for 7 days while covered with a plastic sheet and sprayed with tap water occasionally to keep the specimen surface wet. Thereafter, the specimens were left for curing under indoor conditions for about three months before testing.

All tests were conducted in four consecutive days. The compressive strength of concrete was obtained from compression tests of cylinders, which were conducted following ASTM C39 [29] and using a universal test machine with a load capacity of 5000 kN. The cylinder specimens were first capped using high strength gypsum to ensure that the top and bottom faces were parallel. Each specimen was instrumented with two linear variable displacement transducers (LVDTs) for measuring axial shortenings of the 150 mm mid-height region, and two 80 mm circumferential strain gauges at the mid-height for measuring hoop strains. In addition, two 100 mm axial strain gauges centred at the mid-height were installed mainly for monitoring the concentricity of loading during the initial loading stage. All the three pairs of sensors were installed at 180^o apart around the circumference. The specimens were tested under a displacement loading rate of 0.18 mm/min until the load had dropped to 20% of its peak value. The data from the tests for the compressive strength also allowed the modulus of elasticity and Poisson's ratio of the concrete in compression to be determined according to ASTM C469 [30].

Splitting tests of cylinder specimens were conducted following ASTM C496 [31] and using the same universal test machine as for the cylinder compression tests. Two pieces of thin plywood bearing strips, which had a thickness of 3.0 mm, a width of 25.0 mm and a length slightly longer than the specimen, were bonded to the specimen to distribute the applied load. A diametrical compressive force distributed along the length of the cylinder was applied, and the resulting nominal splitting tensile stress, f_{ts}, can be obtained from the applied load, P, using the following equation:

$$f_{ts} = \frac{2P}{\pi l d} \tag{1}$$

where l and d are the length and diameter of the specimen respectively. The loading was applied at 1.2 MPa/min for the above nominal splitting tensile stress until failure. The splitting tensile strength, $f_{ts,u}$, is determined from the maximum load recorded at failure using Eq. (1).

The flexural performance of the concrete was studied following ASTM C1609 [25] using the four-point bending test of small prismatic beams. A 500 kN electro-hydraulic servo test machine was used. The applied load was equally distributed through a steel loading frame to two loading points. A load cell was installed under each loading point

to monitor the load applied onto each. A roller was used at each support to reduce the friction between the contact surfaces. The rollers might not have completely eliminated the friction between the contact surfaces but the effect is expected to be small [see Fu et al. [32] for a detailed discussion of the issue and how the maximum possible effect can be evaluated]. A rectangular jig was attached to the beam and two LVDTs were installed onto the jig to measure the net deflections at the two sides of the beam at the mid-span (Figure 3). The specimen was loaded under displacement control at a rate of 0.05 mm/min until the mid-span deflection had reached 4.5 mm, which is larger than 1/150 of the beam span as prescribed by ASTM C1609 [25].

The flexural performance of prismatic concrete beams is evaluated using parameters derived from the load-deflection curve. These parameters include the specimen toughness and information at three key points on the load-deflection curve: at the peak load, and at the deflections of 1/600 and 1/150 of the beam span. The load values at these points are denoted as follows: load P_p and the corresponding deflection δ_p at the peak load; loads P_{600} and P_{150} respectively at the deflections of 1/600 and 1/150 of the beam span. The flexural strengths at these three key points are denoted by f_p (= peak strength) and f_{600} and f_{150} (= residual strengths respectively at the deflections of 1/600 and 1/150 of the beam span). The flexural strength is determined from the corresponding load using the following equation:

$$f=PL/bd^2 \tag{2}$$

in which P and f are the load and the corresponding flexural strength; b and d are the average width and depth of the specimen at fracture, respectively. The specimen toughness, T_{150}, is defined as the area under the load-deflection curve with the deflection up to $L/150$.

Results and Discussions

Workability of fresh concrete

The workability of fresh concrete with recycled macro fibres was measured using the slump test. Before casting the specimens, the slump test was conducted three times for each mix (in a single batch). The test results are shown in Table 2 and Figure 4. It is clear that the slump reduced almost linearly with the increase of macro fibre content. Similar to other types of fibre reinforced concrete, the addition of macro fibres increases the total surface area that needs to be coated by a water film, leading to a reduction of free water for cement hydration. The presence of fibres also increases the shear strength of fresh concrete. Both factors result in a reduction of the slump. Optimization of the mix design, such as including superplasticizer, fly ash and a higher amount of macro fibres, may be required for practical applications, but it is beyond the scope of this paper.

Visual examinations indicated that no segregation occurred during the mixing and placing of the four concrete mixes.

Failure modes and properties in compression

The failure modes of the cylinders tested under compression are shown in Figure 5. The control group specimens (without macro fibres) failed with a small number of wide cracks and several large pieces spalling off (Figure 5a), while specimens with macro fibres retained its integrity better with fewer large pieces of concrete spalling off (Figure 5b). The macro fibres in the concrete bridged cracks and constrained the relative sliding of macro shear crack faces, thus resulting in a more distributed crack pattern and a more gradual failure process. Such a trend became more prominent when the macro fibre content increased.

The key compression test results are presented in Table 3, which includes the compressive strength, the axial strain corresponding to the compressive strength, the modulus of elasticity in compression and the Poisson's ratio. Compared with the control specimens, the addition of macro fibres enhanced only very slightly the compressive strength: by 4.4%, 3.9% and 3.6% for the concretes with 0.5%, 1.0% and 1.5% macro fibres respectively. Specially, the highest compressive strength was observed in the concrete with a 0.5% macro fibre content; a further increase in the content of macro fibres led to a very small reduction in the compressive strength. This phenomenon is similar to what was observed by Yazdanbakhsh et al.[18], in which a moderate dosage of FRP needles increased slightly the compressive strength compared with the control specimens without FRP needles, but this increase became smaller when the dosage of the FRP needles further increased. This phenomenon may be explained as follows. The macro fibres in the concrete have three effects: (1) absorbing a small amount of free water and thus slightly decreasing the water/cement ratio [33]; (2) constraining the development of cracks [34,35]; (3) introducing weak interfaces between the macro fibres and concrete. When the former two effects dominate, an increase in the compressive strength would be observed; otherwise a reduction would be evident. The effects of macro fibres on the elastic modulus and the Poisson's ratio are small with the maximum differences (i.e., between the largest value and the smallest one) being 3.4% and 1.4% respectively.

Figure 6 shows the compressive stress-strain curves of the test specimens, in which the axial strain was calculated from the average readings of the two LVDTs divided by the gauge length, and the compressive stress was converted from the applied compressive load divided by the cross-sectional area of the specimen. Clearly, the ascending branches of the compressive stress-strain curves of different concrete groups are almost the same, showing that the small amount of macro fibres (≤1.5% in volume) had a negligible effect on the elastic modulus of the concrete. The effect was more prominent

on the post-peak softening behaviour, because the macro fibres could bridge the wing-cracks and therefore cause a more gradual descending branch. The softening process tends to be more gradual in general when the concrete contains more macro fibres [35,36]. The differences between the descending branches of the specimens in the same group are large, which is similar to that observed in Kazmi et al. [35]. Such a large scatter in the descending branch may be mainly attributed to the inherent random nature of both concrete cracking and distribution of macro fibres.

Splitting failure modes and tensile properties

Figure 7 shows two typical splitting failure modes respectively for specimens of the control group and those with macro fibres. The specimens of the control group, which had no macro fibres, broke suddenly into two halves along the loaded diametrical plane at the peak load. By contrast, the specimens with macro fibres could continue to resist a higher load after the appearance of the major crack because of the bridging effect of macro fibres. They were eventually split into two halves with many bridging fibres seen. After the appearance of the splitting crack, noises due to either macro fibre rupture or pull-out were continuously emitted. An inspection of the failed specimens did confirm that some macro fibres were pulled out from the concrete (Figure 7b).

The splitting tensile strength test results are shown in Table 4 and Figure 8. When the macro fibre volume fraction increased from 0 to 0.5%, 1.0% and 1.5%, the average splitting tensile strength of concrete was significantly enhanced from 3.19 MPa to 3.87 MPa, 4.12 MPa and 4.86 MPa, respectively, i.e., an increase of 21%, 29% and 52% respectively. Figure 8 shows that the splitting tensile strength increases approximately linearly with the increase of macro fibre volume fraction, suggesting that the enhancement in splitting tensile strength could be even higher if the volume fraction of macro fibres was further increased. Clearly, the addition of macro fibres in the concrete mix has a much greater beneficial effect on the splitting tensile strength than the compressive strength. This is consistent with the behaviour of concrete reinforced with other types of fibres, and shows that the macro fibres were more effective in constraining the development of Mode I cracks than other types of cracks.

Flexural failure modes and properties

Figure 9 shows the failure modes of all the beam specimens tested in flexure. All specimens failed by the formation and development of a major flexural crack in the constant moment region. The reference specimens broke suddenly into two pieces very shortly after the appearance of a major flexural crack. The MFRC specimens failed in a more ductile manner, which is similar to the failure mode of two-way concrete slabs with macro polypropylene fibers observed by Ding et al. [37]. The load increased

continuously after the appearance of the major crack, and then dropped gradually after the peak. Some noises of macro fibre rupture or pull-out were heard during the failure process. The two halves of an MFRC specimen were still connected by some macro fibres after failure.

Figure 10 shows the load-deflection curves of all the beam specimens, in which the load is the average of the two load cell readings, and the deflection is the average of the two LVDT readings. All the curves start with a linear ascending branch, representing the load-deflection curve before the cracking of concrete. The stiffness of the linear ascending branch is almost the same for all specimens, indicating that the presence of macro fibres had little effect on the elastic modulus of concrete. After the appearance of a major crack, the macro fibres started to be mobilized to resist tensile forces and bridge the crack, leading to further increases in load (hardening) and then large deformations after the peak load (softening). Large differences are apparent in both the strength and the descending branch of the beam specimens, which are mainly attributed to the randomness of concrete cracking behaviour as well as the number and distribution of macro fibres across the major crack.

The load-deflection curves may be classified into three patterns as shown in Figure 11. Pattern I represents the curves of the reference specimens, characterized by an abrupt drop in the load to zero immediately after the appearance of the major flexural crack. Because the load dropped suddenly, so the post-peak curves of these specimens are not available.

Three of the four specimens of the MFRC0.5 group had a load-deflection curve of Pattern II, which has the same strength as the reference specimens and is further characterized by a softening branch following a linear ascending branch. At the initiation of the major flexural crack, part of the tensile force resisted by the lower part of concrete in the beam was released. The released tensile force had to be taken up by the macro fibres across the crack. Due to the low fibre content, the number of fibres was small so these fibres either gradually debonded from concrete or ruptured immediately after the appearance of the major crack. It may be noted that one of the specimens in this group exhibited an ascending branch after the initiation of the major crack, probably because the distribution of macro fibres across the crack in this specimen was more advantageous than that in the other three specimens.

Specimens with a higher macro fibre content (i.e., the MFRC1.0 and MFRC1.5 groups) exhibited a load-deflection curve of Pattern III, which is characterized by a hardening branch following a linear ascending branch. Note that the presence of fibres did not affect the cracking load. A relatively large number of macro fibres crossing the crack in these specimens meant that they could resist the entire tensile force released by the cracked concrete, and in addition had the capacity to allow the applied load to increase

further. After the peak load, the macro fibres crossing the crack started to debond or rupture, resulting in the softening branch of the load-deflection curve.

The key flexural test results are summarized in Table 5. It should be noted that the results of some specimens were excluded from calculating the average values as the ultimate loads of these specimens (i.e., outlier specimens) deviate by more than 20% from the average value of all specimens of the same group. As seen in Table 5, it is more likely to have such an outlier case when the specimen is more susceptible to large random variations in the number and distribution of macro fibres due to a relatively small number of macro fibres in the specimen. The average flexural strengths were 6.40 MPa, 10.11 MPa and 12.18 MPa respectively for MFRC specimens with 0.5%, 1.0% and 1.5% macro fibres; these are 16%, 83% and 135% higher than that of the reference beams respectively. The residual flexural strengths at deflections of 1/600 and 1/150 of the span (i.e., f_{600} and f_{150}) also increased with an increase in the fibre content. For all specimens in the MFRC0.5, MFRC1.0 and MFRC1.5 groups, the average values for f_{600} were 4.47 MPa, 9.12 MPa and 10.85 MPa respectively, and for f_{150} are 2.09 MPa, 4.08 MPa, and 5.14 MPa respectively. These are substantially higher compared with the corresponding values of 0.21 MPa and 0.16 MPa respectively for the control specimens. Similarly, the average toughness of the specimens in the control group was only 0.97 J, while the average toughness were 82.3 J, 151.3 J, and 182.4 J, for specimens with 0.5%, 1.0% and 1.5% macro fibres, respectively. Therefore, it can be concluded that the flexural performance, including the flexural strength, deformation capacity and toughness, were significantly improved by the incorporation of macro fibres; and the enhancement was more significant when the volume fraction of macro fibres was higher.

Conclusions

This paper has explored a novel mechanical recycling method for FRP wastes in which waste FRP components are processed into macro fibres for use as distributed reinforcing elements in concrete. The effects of incorporating macro fibres into concrete on the mechanical properties of concrete have been investigated through compression, splitting and bending tests. The following conclusions can be drawn from the results and discussions presented in the paper:

- The addition of macro fibres significantly reduced the workability of concrete, but the concrete incorporating macro fibres of 1.5% in volume still had a slump of over 80 mm without adding any superplasticizer.
- The compressive strength of concrete increased slightly, by up to 4.4%, as a result of including no more than 1.5% macro fibres into the concrete. The descending branch of the compressive stress-strain curve tended to become more gradual with the addition of macro fibres, so a higher toughness resulted from a higher dosage of macro fibres.

- The splitting tensile strength increased approximately linearly with the increase of macro fibre content. The concrete with a 1.5% macro fibre content achieved an average splitting tensile strength of 4.86 MPa, which is 52% higher than that of the reference specimens without macro fibres.
- The addition of macro fibres resulted in a significant enhancement of the flexural performance of concrete beams, including the peak strength, the residual strength as well as the toughness. Concrete beams with a 1.5% macro fibre content showed average values of strength and toughness that are 1.3 and 230 times those of specimens in the control group.
- A large scatter was observed in the test results of specimens of the same group, which is mainly attributed to the inherent random nature of both the number and distribution of macro fibres. Specimens with a relatively small number of macro fibres are more susceptible to random variations in the number and distribution of macro fibres and hence the test results.
- All prismatic beam specimens failed by the formation and development of a major crack in the constant moment region. The specimens with macro fibres failed in a more ductile manner than those in the control group. The load-deflection curves of control specimens are characterized by an abrupt drop in the load to zero following a linear ascending branch up to the cracking of concrete, while those specimens with macro fibres showed either a hardening or a softening branch following a linear ascending branch.

Acknowledgements

The authors gratefully acknowledge the financial support provided by the Hong Kong Research Grants Council (Project No: T22-502/18-R), The Hong Kong Polytechnic University (Project Account Code: 1-BBAG), and the National Natural Science Foundation of China (Project Nos: 51608130 and 51978176). The authors also wish to thank Mr. Huang Jun-Jian for his help in conducting some of the tests and Techstorm Advanced Materials Co. Ltd. for providing the decommissioned wind blade used in this study.

References

[1] Teng, J.G., Chen, J.F., Smith, S.T. and Lam, L. (2002). *FRP-strengthened RC Structures*, West Sussex: Wiley.

[2] Witten, E., Jahn, B. and Karl, D. (2015). *Composites Market Report 2015*. Carbon Composites/AVK.

[3] Jacob, A. (2011). Composites can be recycled. *Reinforced Plastics*, 55(3), 45-46.

[4] Oliveux, G., Dandy, L. and Leeke, G. (2015). Current status of recycling of fibre reinforced polymers: Review of technologies, reuse and resulting properties. *Progress in Materials Science*, 72, 61-99.

[5] Job, S., Leeke, G., Mativenga, P.T., Oliveux, G. Pickering, S. and Shuaib, N.A. (2016). *Composite Recycling: Where Are We Now?* Composites UK Ltd.

[6] Yazdanbakhsh, A. and Bank, L.C. (2014). A critical review of research on reuse of mechanically recycled FRP production and end-of-life waste for construction. *Polymers*, 6(6), 1810-1826.

[7] EC Directive (2018), Directive 2018/850/EU of the European Parliament and of the Council of 30 May 2018 amending Directive 1999/31/EC on the landfill of waste, *Official Journal of the European Union*, L150, 100-108.

[8] Fabian, N and Lou, L.I.T. (2019). The struggle for sustainable waste management in Hong Kong: 1950s–2010s. *Worldwide Waste: Journal of Interdisciplinary Studies*, 2(1): 1–12.

[9] European Composites Industry Association (2011). *Glass fibre reinforced thermosets: recyclable and compliant with the EU legislation*, EuCIA position paper 52816.

[10] Plastics.gl (2014). *Waste FRP Recycling*, accessed on 21 June 2019, https://www.plastics.gl/processing-misc/waste-frp-recycling/.

[11] Asokan, P., Osmani, M. and Price, A.D.F. (2009). Assessing the recycling potential of glass fibre reinforced plastic waste in concrete and cement composites. *Journal of Cleaner Production*, 17(9), 821-829.

[12] Correia, J.R., Almeida, N.M. and Figueira, J.R. (2011). Recycling of FRP composites: reusing fine GFRP waste in concrete mixtures. *Journal of Cleaner Production*, 19(15), 1745-1753.

[13] Huang, Z., Ge, H., Zhao, Y., Liu, F.G. and Yin, J.J. (2016). Reuse FRP waste as filler replacement for sisal fiber reinforced sheet molding compound. *Polymer Composites*, 39(6), 1896-1904.

[14] García, D., Vegas, I. and Cacho, I. (2014). Mechanical recycling of GFRP waste as short-fiber reinforcements in microconcrete. *Construction and Building Materials*, 64, 293-300.

[15] Farinha, C.B., de Brito, J. and Veiga, R. (2018). Assessment of glass fibre reinforced polymer waste reuse as filler in mortars. *Journal of Cleaner Production*, 210, 1579-1594.

[16] Tittarelli, F. and Shah, S.P. (2013). Effect of low dosages of waste GRP dust on fresh and hardened properties of mortars: Part 1. *Construction and Building Materials*, 47, 1532-1538.

[17] Yazdanbakhsh, A., Bank, L. and Chen, C. (2016). Use of recycled FRP reinforcing bar in concrete as coarse aggregate and its impact on the mechanical properties of concrete. *Construction and Building Materials*, 121, 278-284.

[18] Yazdanbakhsh, A., Bank, L.C., Chen, C. and Tian, Y. (2017) FRP-needles as discrete reinforcement in concrete. *Journal of Materials in Civil Engineering*, ASCE, 29(10), Article No.: 04017175

[19] Alam, S.M., Slater, E. and Billah, A.H.M.M. (2013). Green concrete made with RCA and FRP scrap aggregate: Fresh and hardened properties. *Journal of Materials in Civil Engineering*, 25(12), 1783-1794.

[20] Yazdanbakhsh, A., Bank, L.C., Rieder, K.A., Tian, Y. and Chen, C. (2018a). Concrete with discrete slender elements from mechanically recycled wind turbine blades. *Resources Conservation and Recycling*, 128, 11-21.

[21] Yazdanbakhsh, A., Bank, L.C. and Tian, Y. (2018b). Mechanical processing of GFRP waste into large-sized pieces for use in concrete. *Recycling*, 3(1), 8.

[22] Dong, Z.Q., Wu, G. and Zhu, H. (2019). Mechanical properties of seawater sea-sand concrete reinforced with discrete BFRP-Needles. *Construction and Building Materials*, 206, 432-441.

[23] Nie, X.F., Fu, B., Teng, J.G., Bank, L.C., Tian, Y. (2020). Shear behavior of full-scale reinforced concrete beams with GFRP needles, *Construction and Building Materials*, 257, Article ID: 119430.

[24] ACI (2008). "Guide for specifying, proportioning, and production of fiber-reinforced concrete", American Concrete Institute 544, Farmington Hills, MI, USA.

[25] ASTM (2012). "Standard test method for flexural performance of fiber reinforced concrete (using beam with third-point loading)." *ASTM C1609*, West Conshohocken, PA.

[26] ASTM (2015b). "Standard test method for obtaining average residual strength of fiber-reinforced concrete." *ASTM C1399*, West Conshohocken, PA.

[27] Buildings Department (2004). "Code of practice for structural use of concrete 2004", The Government of the Hong Kong Special Administrative Region, China.

[28] ASTM (2015c). "Standard test method for slump of hydraulic-cement concrete." *ASTM C143*, West Conshohocken, PA

[29] ASTM (2015a). “Standard test method for compressive strength of cylindrical concrete specimens.” *ASTM C39*, West Conshohocken, PA.

[30] ASTM (2014). “Standard test method for static modulus of elasticity and Poisson’s ratio of concrete in compression.” *ASTM C469*, West Conshohocken, PA.

[31] ASTM (2011). “Standard test method for splitting tensile strength of cylindrical concrete specimens.” *ASTM C496*, West Conshohocken, PA.

[32] Fu, B., Teng, J.G., Chen, G.M. Chen, J.F. and Guo, Y.C. (2018). Effect of load distribution on IC debonding in FRP-strengthened RC beams: Full-scale experiments. *Composite Structures*, 188, 483-496.

[33] Yang, Q., Xian, G. and Karbhari, V.M. (2008). Hygrothermal ageing of an epoxy adhesive used in FRP strengthening of concrete. *Journal of Applied Polymer Science*, 107(4), 2607-2617.

[34] Li, V.C. (1992). Simplified micromechanical model of compressive strength of fiber-reinforced cementitious composites. *Cement and Concrete Composite*, 14(2), 131-141.

[35] Kazmi, S.M.S., Munir, M.J., Wu, Y.F. and Patnaikuni, I. (2018). Effect of macro-synthetic fibers on the fracture energy and mechanical behavior of recycled aggregate concrete, *Construction and Building Materials*, 189, 857-868.

[36] Kazmi, S.M.S., Munir, M.J., Wu, Y.F., Patnaikuni, I., Zhou, Y. and Xing, F. (2019). Axial stress-strain behavior of macro-synthetic fiber reinforced recycled aggregate concrete. *Cement and Concrete Composites*, 97, 341-356.

[37] Ding, Y., Wang, Q., Pacheco-Torgal, F. and Zhang, Y. (2020). Hybrid effect of basalt fiber textile and macro polypropylene fiber on flexural load-bearing capacity and toughness of two-way concrete slabs. *Construction and Building Materials*, 261, Article ID: 119881.

Table 1. Concrete mix proportions (kg/m^3)

Component	Mixture			
	CC	MFRC0.5	MFRC1.0	MFRC1.5
Cement	539			
Water	255			
River sand	610			
Coarse aggregate	996			
Recycled macro fibers	0	9.85	19.70	29.55
Volume ratio of recycled macro fibers	0	0.5%	1.0%	1.5%

Table 2. Slump of each concrete mixture (mm)

Type	Test No.			
	1	2	3	average
CC	178	175	174	176
MFRC0.5	152	142	137	144
MFRC1.0	116	108	109	111
MFRC1.5	83	85	81	83

Table 3. Key results of compression tests

Type	Specimen No.	f_c (MPa)	$f_{c,m}$ (MPa)	ε_{co} (%)	$\varepsilon_{co,m}$ (%)	E (GPa)	E_m (GPa)	v	v_m
CC	1	45.1	45.7	0.259	0.265	29.6	29.2	0.217	0.215
	2	46.4		0.274		29.1		0.207	
	3	45.8		0.279		28.6		0.220	
	4	45.5		0.249		29.5		0.215	
MFRC0.5	1	47.5	47.7	0.286	0.270	29.6	30.2	0.220	0.215
	2	47.2		0.272		31.4		0.226	
	3	47.5		0.269		28.2		0.198	
	4	48.8		0.253		31.8		0.216	
MFRC1.0	1	48.4	47.5	0.281	0.269	28.5	30.2	0.208	0.217
	2	47.8		0.293		30.8		0.232	
	3	47.0		0.259		30.6		0.214	
	4	46.9		0.243		30.9		0.216	
MFRC1.5	1	47.8	47.4	0.301	0.284	28.3	29.6	0.212	0.214
	2	48.2		0.286		30.7		0.193	
	3	47.6		0.283		30.7		0.231	
	4	45.8		0.267		28.8		0.220	

Note: f_c – compressive strength; ε_{co} – strain at compressive strength; E – modulus of elasticity in compression; v – Poisson's ratio; $f_{c,m}$, $\varepsilon_{co,m}$, E_m and v_m – mean values.

Table 4. Splitting tensile strength, $f_{ts,u}$ (MPa)

Type	Specimen No.				
	1	2	3	4	average
CC	3.11	3.77	2.80	3.08	3.19
MFRC0.5	3.85	3.69	3.94	4.01	3.87
MFRC1.0	4.49	3.90	3.87	4.24	4.12
MFRC1.5	4.40	4.98	4.59	5.45	4.86

Table 5. Key results of four-point bending tests

No.	Peak load P_p (kN)	strength f_p (MPa)	Deflection at peak load δ_P (mm)	Residual load P_{600} (kN)	Residual load P_{150} (kN)	Residual strength f_{600} (MPa)	Residual strength f_{150} (MPa)	Toughness T_{150} (J)
CC-1	32.7	5.33	0.05	0.00	0.62	0.00	0.10	0.98
CC-2	34.0	5.54	0.05	2.19	0.99	0.36	0.16	0.84
CC-3	35.1	5.72	0.05	1.72	1.31	0.28	0.21	1.09
Mean	**34.0**	**5.53**	**0.05**	**1.30**	**0.97**	**0.21**	**0.16**	**0.97**
MFRC0.5-1	42.3	6.89	0.45	34.0	22.5	5.53	3.66	113.1
MFRC0.5-2	36.2	5.90	0.06	20.9	3.2	3.40	0.52	51.6
MFRC0.5-3	65.2*	10.63*	0.46*	46.5*	6.4*	7.57*	1.05*	90.5*
MFRC0.5-4	30.6*	4.99*	0.05*	17.8*	7.0*	2.91*	1.14*	48.5*
Mean	**39.3**	**6.40**	**0.25**	**27.4**	**12.8**	**4.47**	**2.09**	**82.3**
MFRC1.0-1	65.9	10.74	0.31	64.6	23.8	10.53	3.87	158.0
MFRC1.0-2	62.8	10.23	0.79	61.9	34.5	10.08	5.62	174.3
MFRC1.0-3	48.1*	7.84*	0.31*	38.7*	25.8*	6.31*	4.20*	135.1*
MFRC1.0-4	71.4	11.64	0.58	58.6	16.2	9.54	2.63	137.9
Mean	**62.1**	**10.11**	**0.56**	**55.9**	**25.1**	**9.12**	**4.08**	**156.7**
MFRC1.5-1	60.0*	9.75*	0.33*	45.9*	18.7*	7.50*	3.05*	115.9*
MFRC1.5-2	76.5	12.45	0.68	69.5	31.5	11.33	5.14	187.4
MFRC1.5-3	81.5	13.28	0.44	74.0	31.1	12.06	5.06	205.7
MFRC1.5-4	81.3	13.25	0.61	76.7	44.7	12.49	7.29	220.9
Mean	**79.8**	**12.18**	**0.58**	**66.5**	**31.5**	**10.85**	**5.14**	**204.6**

Notes:

P_{600}=Residual load at mid-span deflection of L/600; P_{150}=Residual load at mid-span defection of L/150; f_{600}=Residual strength at mid-span deflection of L/600; f_{150}=Residual strength at mid-span deflection of L/150; T_{600}=Area under the load-deflection curve from 0 to L/150.

* The value of this specimen was excluded from calculating the mean value as its ultimate load deviates by more than 20% from the average of the same group, and seems to be unreliable possibly due to an unreasonable number and distribution of macro fibers.

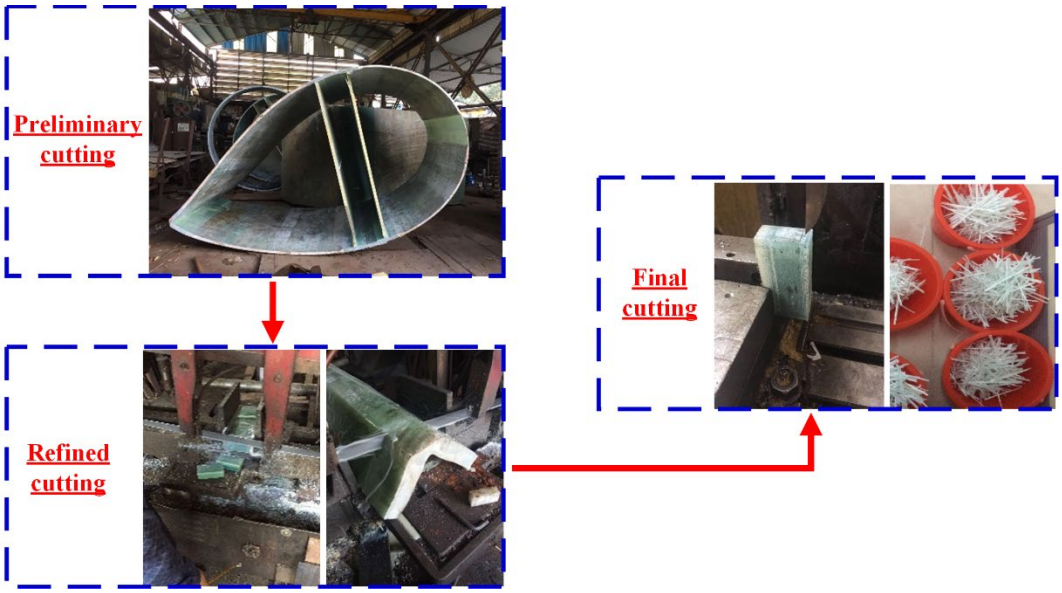

Figure 1 Mechanical processing of a wind turbine blade into macro fibres

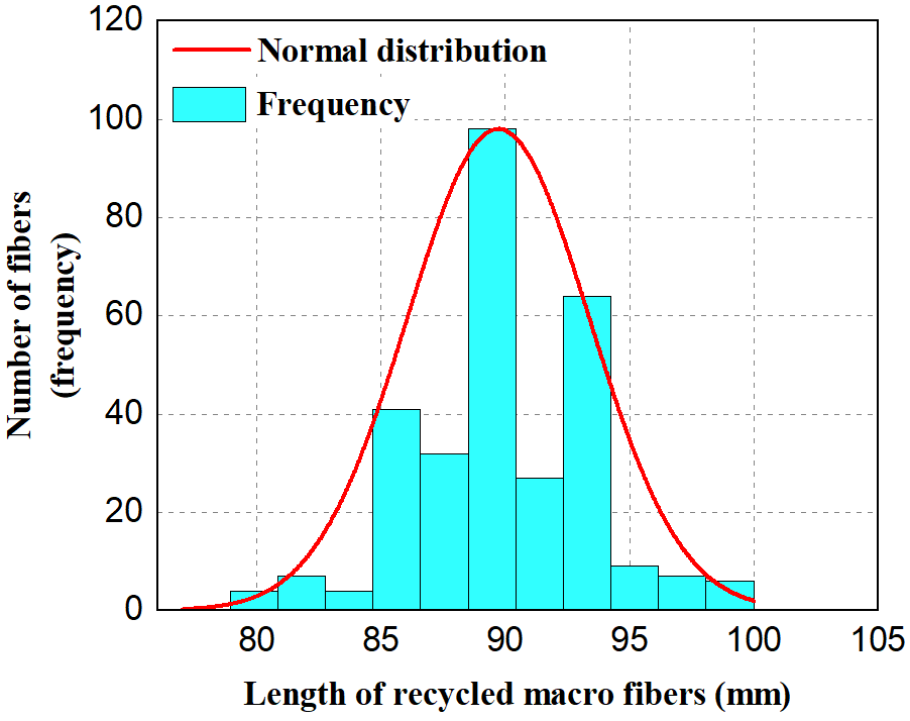

(*a*) length

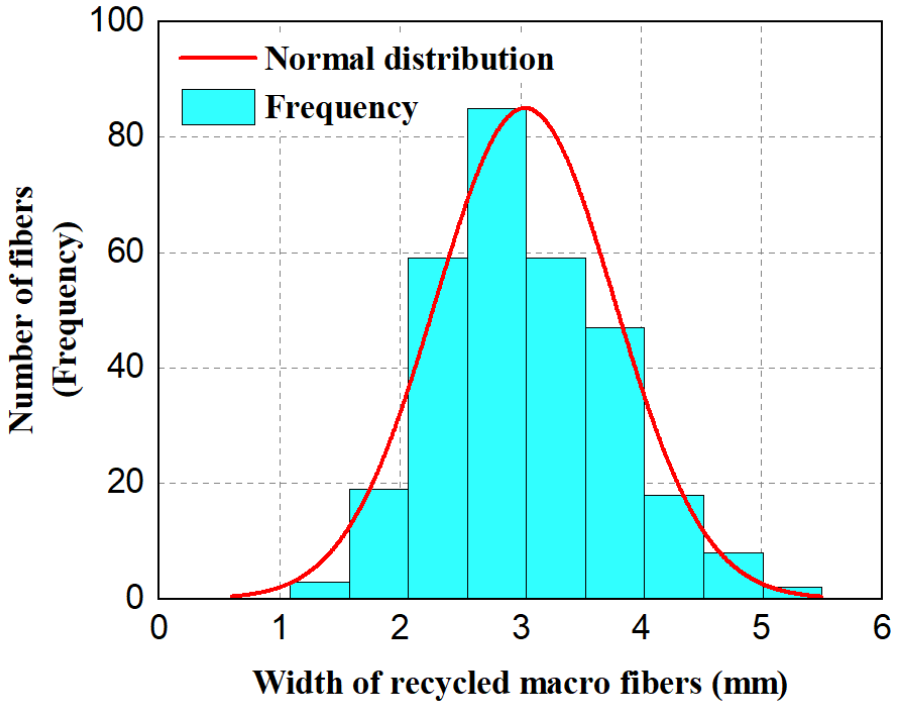

(*b*) width

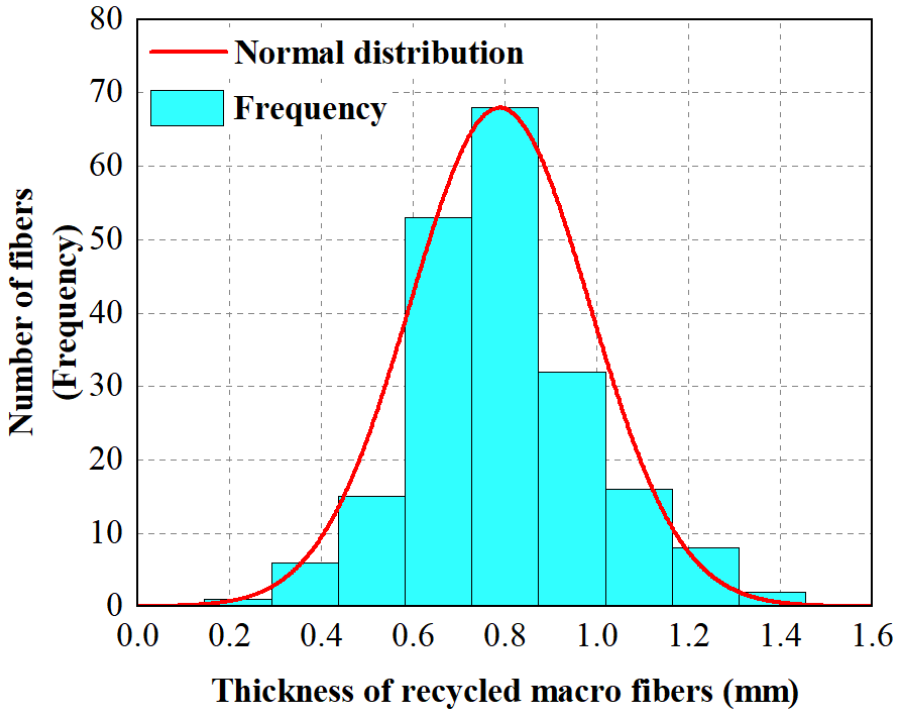

(*c*) thickness

Figure 2 Statistical characteristics of recycled macro fiber dimensions: (*a*) length; (*b*) width; (*c*) thickness

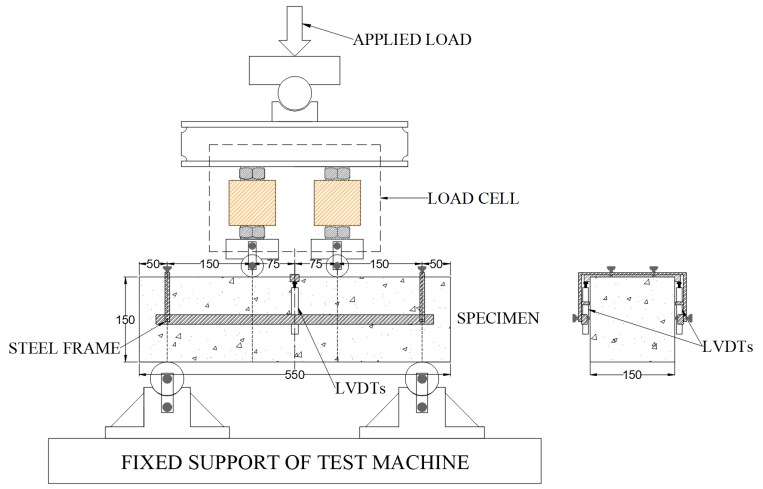

(*a*)

(*b*)

Figure 3 Experimental set-up for four-point bending tests: (*a*) schematic (*b*) test in progress

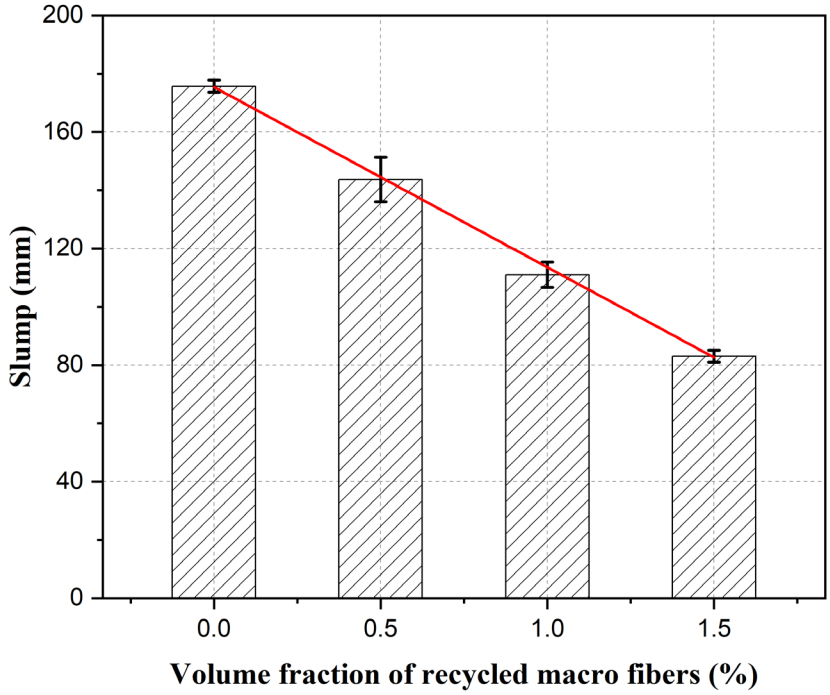

Figure 4 Effect of volume ratio of macro fibers on concrete slump

(*a*)

(*b*)

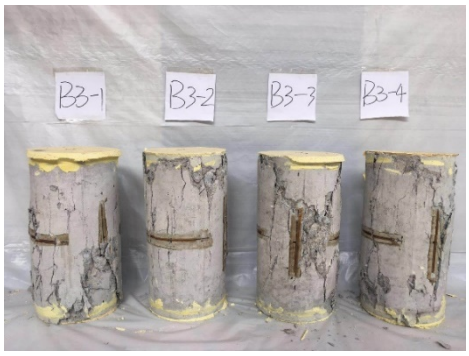

(c)

(d)

Figure 5 Compression failure modes of cylinder specimens: (a) CC; (b) MFRC0.5; (c) MFRC1.0; (d) MFRC1.5

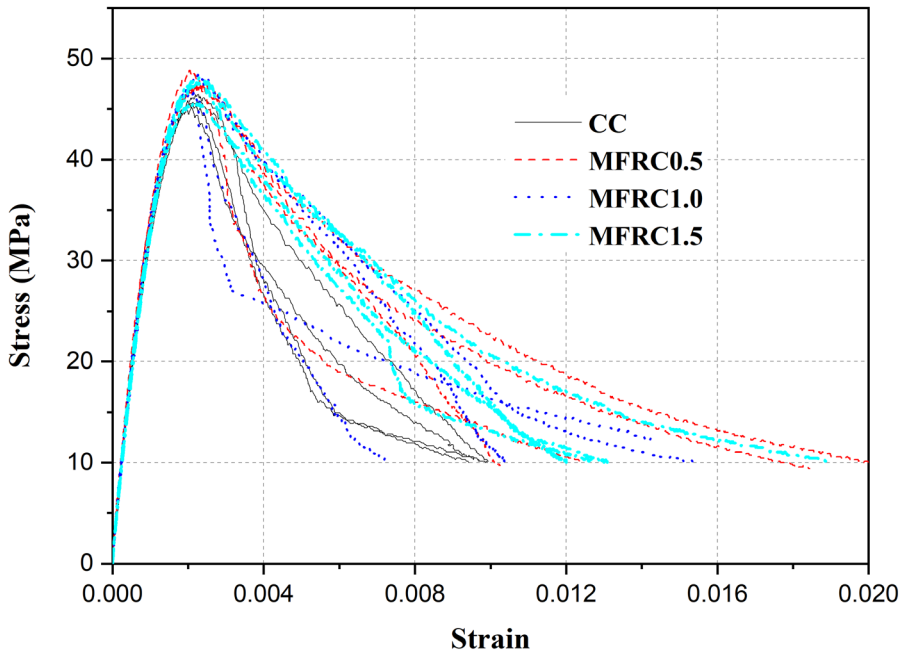

Figure 6 Compressive stress-strain curves

(*a*) (*b*)

Figure 7 Typical splitting failure modes: (*a*) reference specimens; (*b*) MFRC specimens

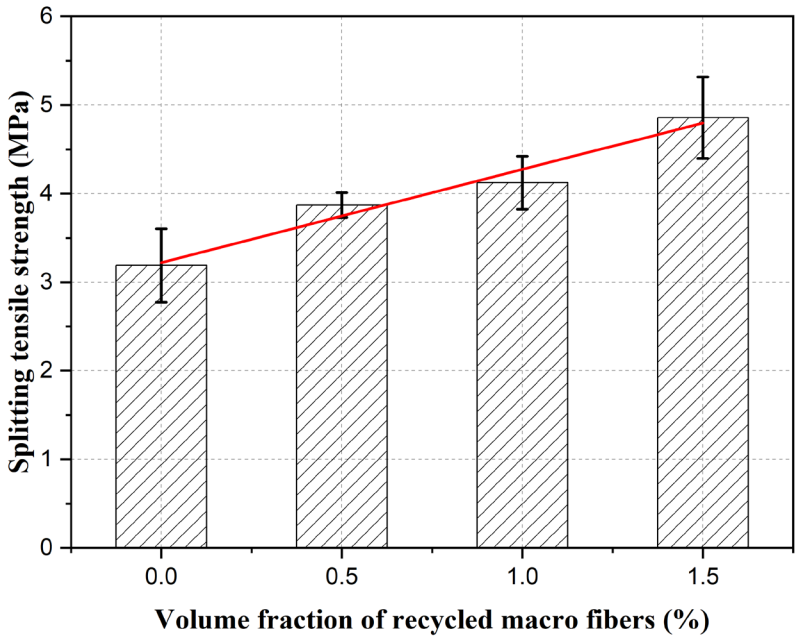

Figure 8 Effect of volume ratio of macro fibers on splitting tensile strength

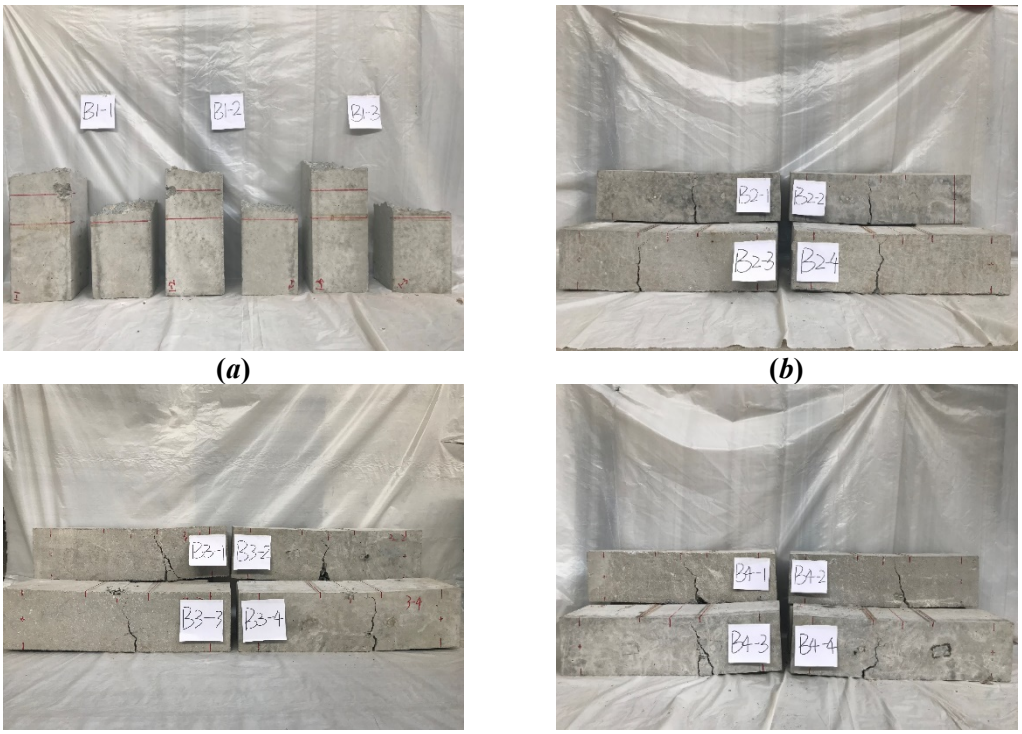

(*a*) (*b*)

(c) (d)

Figure 9 Failure modes of beam specimens tested in four-point bending: (a) CC; (b) MFRC0.5; (c) MFRC1.0; (d) MFRC1.5

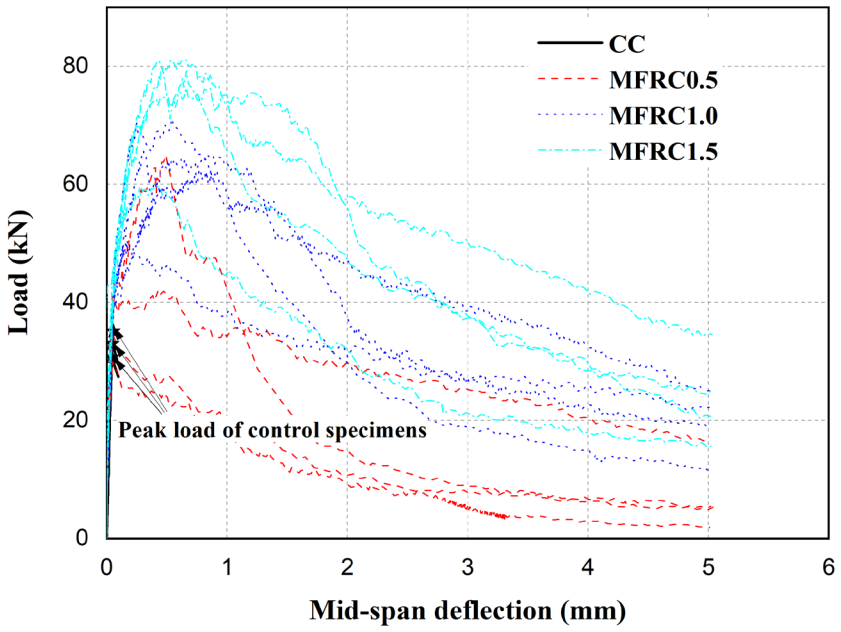

(*a*)

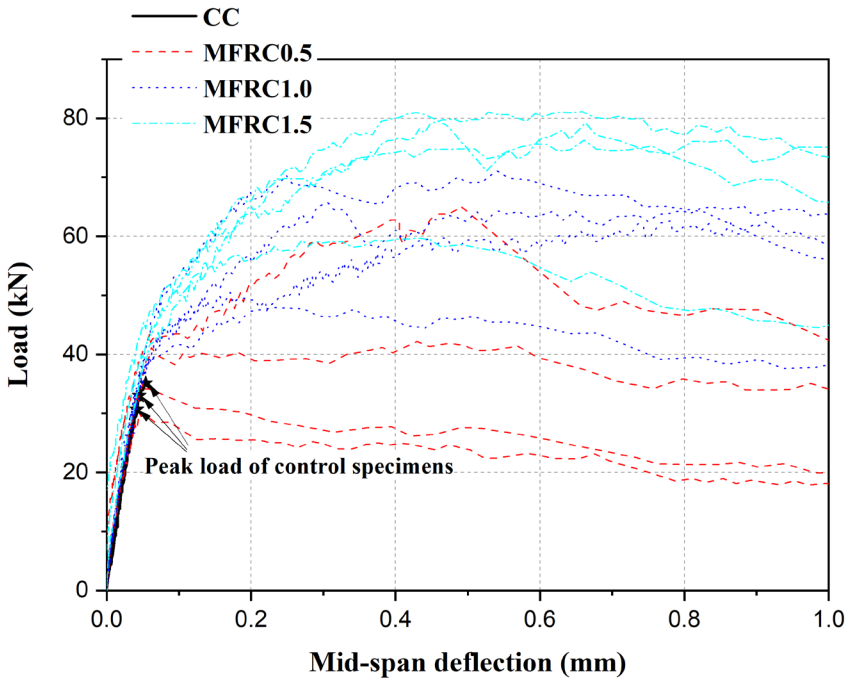

(*b*)

Figure 10 Load-deflection curves of beams tested in four-point bending: (a) full-range curve; (b) initial stage up to a deflection of L/450

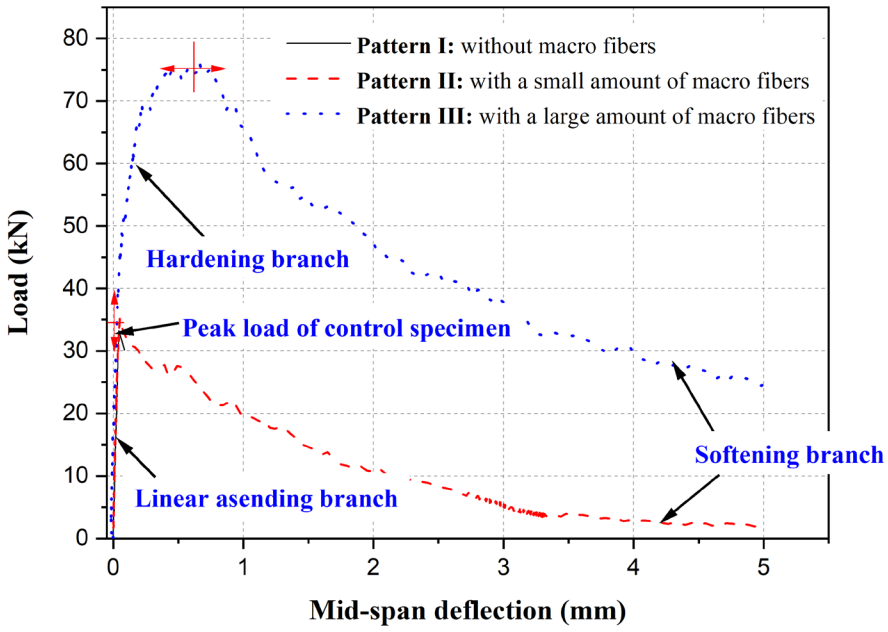

(a)

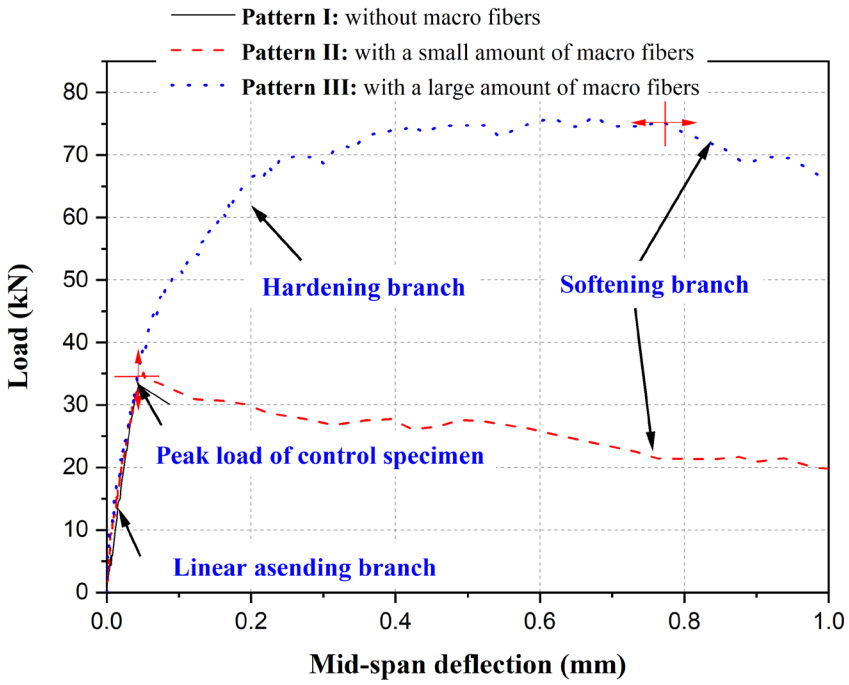

(b)

Figure 11 Typical load-deflection curves of beams tested in four-point bending (a) full-range curve; (b) initial part up to the deflection of L/450